Titanium oxide nanotubes for bone regeneration

SUGURU KUBOTA*, KOHEI JOHKURA, KAZUHIKO ASANUMA, YASUMITSU OKOUCHI, NAOKO OGIWARA, KATSUNORI SASAKI
Department of Anatomy and Organ Technology, Shinshu University, School of Medicine, 3-1-1 Asahi, Matusmoto 390-8621, Japan
E-mail: kub@wondernet.ne.jp

TOMOKO KASUGA
Electrotechnology Applications R&D Center, Chubu Electric Power Co. Inc., Oodaka, Midori-ku, Nagoya 459-8522, Japan

Titanium oxide nanotubes with Ca ions on their surfaces were prepared as 2 mm cylindrical inserts and placed into surgically created bone defects in the femurs of Wistar rats. On day 3, fibroblast-like cells were present on the surface of the nanotube inserts and fibers were observed by scanning electron microscopy (SEM). On day 7, cells with alkaline phosphatase activity were present and identified as osteoblasts by SEM and transmission electron microscopy. New bone matrices were observed in and around the porous nanotube inserts by light microscopy. Compared with clinically used hydroxyapatite and β-tricalcium phosphate, titanium oxide nanotubes promote faster acquisition and development of osteoblasts and bone tissues and have better bone regenerating ability after one week.

1. Introduction

Metallic titanium used in clinical orthopedic biomaterials usually has a thin layer of titanium oxide (TiO_2) on its surface [1]. TiO_2 does not induce morphological transformation in mammalian cells or mutation in bacteria, and it has no known toxic effects on living cells [2]. In orthopedic applications, TiO_2 makes direct contact with bone tissue, and as with other cells, it has good biocompatibility.

TiO_2 promotes the formation of apatite, a major component of bone tissue, on its surface when incubated in a plasma-like solution for 10 days [3, 4]. In 1998 Kasuga *et al*. [5, 6] developed a method for the synthesis of TiO_2 nanotubes composed of needle-shaped crystals. The crystals have a diameter of 8 nm, a length of 100 nm, and a large surface area of about 400 m^2/g. *In vitro*, TiO_2 nanotubes form bone-like apatite crystals in only one day when incubated in simulated plasma (unpublished data). Therefore TiO_2 nanotubes could promote more rapid bone development and augment existing bone repair procedures. The purpose of this study was to compare the efficacy of TiO_2 nanotubes to other clinically-used biomaterials like hydroxyapatite (HA) and β-tricalcium phosphate (β-TCP) in living animals with bony defects.

2. Material and methods

2.1. Animals

Twenty-two 12-week old male Wistar Rats (average weight 275 g) (SLC Inc., Shizuoka, Japan) were used. Eight rats received TiO_2 nanotube inserts, six received HA inserts (Bonfil, Mitusbishi Material Inc., Tokyo, Japan), six received β-TCP inserts (Osferion, Olympus Optical Inc., Tokyo, Japan), and two rats served as controls. The procedures were performed in accordance with the guidelines of animal experimentation of Shinshu University.

2.2. Preparation of inserts

TiO_2 nanotubes were made at Electrotechnology Applications R&D Center of Chubu Electric Power Co. Inc. (Nagoya) in the manner previously described [6]. In this study $Ca(COO)_2$ was used for neutralization instead of HCl. Bonfil and Osferion were molded in glass cylinders of 2.0 mm diameter and 3–5 mm long with the pressure of 1000 kg/cm^2.

Porous TiO_2 nanotubes were made with 1.0 g nanotubes, 0.2 g poly-lactic acid (dissolved with dichloromethane) and 4.0 g NaCl molded in glass cylinders of 2.0 mm diameter with the pressure of 10 kg/cm^2. The NaCl component of this product was dissolved in water, leaving TiO_2 nanotubes inserts that were porous. The porosity was 90%.

2.3. Application of inserts

After anesthesia with pentobarbital sodium (0.07 ml/100 g, i.p.), femurs of rats were exposed through skin incisions. Using a drill with a sterile blade, a hole of 2 mm diameter was made in the mid-diaphysis of the femur. The depth of the hole was about 3 mm and

*Author to whom all correspondence should be addressed.

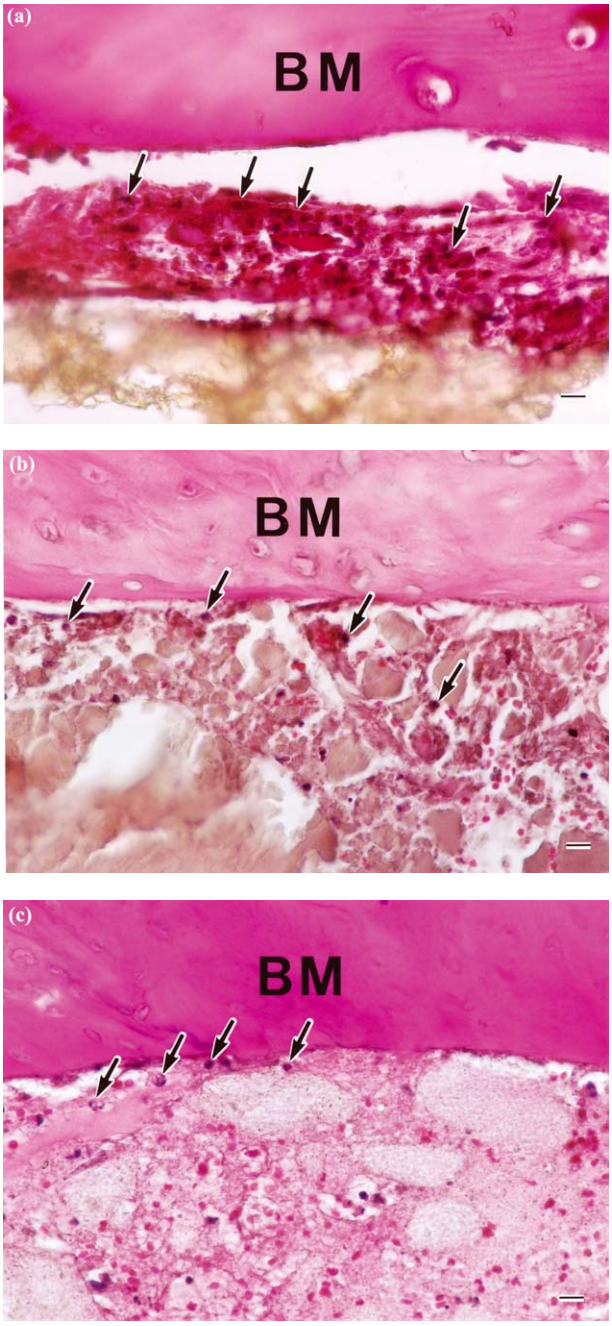

Figure 1 Light microscopy of rat femurs and inserts on the day 3. (a) Non-porous TiO_2 nanotube inserts (lower portion) had fibroblast-like cells (arrows) between the nanotubes and bone matrix (BM). The cells were spindle shaped and well stained. No cells were present within the insert. (b) HA inserts had many fewer cells between the insert and BM than did the TiO_2 nanotube inserts shown in (a). The cells that were present were round shaped leukocyte-like cells (arrows). (c) β-TCP inserts also had very few cells between the insert and BM. Some free, round leukocyte-like cells (arrows), were also present within the insert. (HE staining, bar = 10 μm).

communicated with the bone marrow. Each 2-mm cylinder (TiO_2 nanotubes, HA, β-TCP) was inserted into the hole and the skin sutured over it.

2.4. Morphological studies

On days 3 and 7 after the operation, animals were sacrificed under anesthesia and femurs were removed.

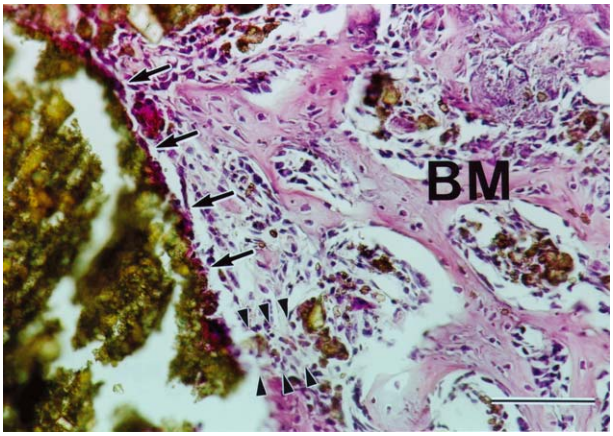

Figure 2 Light microscopy of the porous type TiO_2 nanotube insert and new bone formation on day 7. Cells were located on the outer surfaces (arrows) of the insert and also entered its pores (arrow heads). Newly formed BM had the appearance of normal immature bone. (HE staining; bar = 100 μm).

2.4.1. Light microscopy

The paraformaldehyde-fixed tissue sections were decalcified for a few days in K-CX decalcification solution (Fujisawa Pharmaceutical Co., Ltd., Osaka, Japan). Thin sections (10 μm) were stained with hematoxylin and eosin or with nitro-blue-tetrazolium chlorid/bromo-chloro-3-indolyl-phosphate (NBT/BCIP) (Bio-Rad Lab, USA) for alkaline phosphatase activity.

2.4.2. Electron microscopy

Bones with inserts were fixed in 45 mM cacodylate buffer solution containing 2.5% glutaraldehyde for 24 h and were washed with 45 mM cacodylate buffer containing 180 mM sucrose. For scanning electron microscopy (SEM), tissues were postfixed with 1% O_sO_4 cacodylate buffer solution for overnight and were dehydrated in a graded ethanol series. Specimens were immersed in isoamyl acetate for 30 min and then dried using the critical point method. They were coated to a thickness of 5 nm with an osmium plasma coator (Nippon Laser, Nagoya, Japan) and observed with a JSM 6000-F (JOEL, Tokyo, Japan) electron microscope at an accelerating voltage of 15 kV.

For freeze cracking, the tissue was immersed in 70%

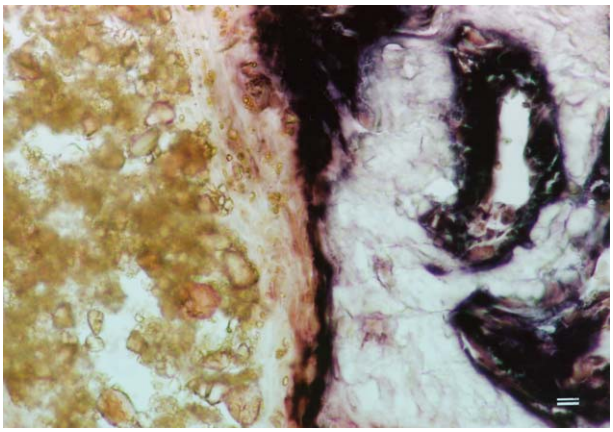

Figure 3 Light microscopy of TiO_2 nanotube porous inserts and bone matrix with alkaline phosphatase stain on day 7. Alkaline phosphatase positive cells were present beside the nanotubes. On the opposite side of the cells was newly formed BM (bar = 10 μm).

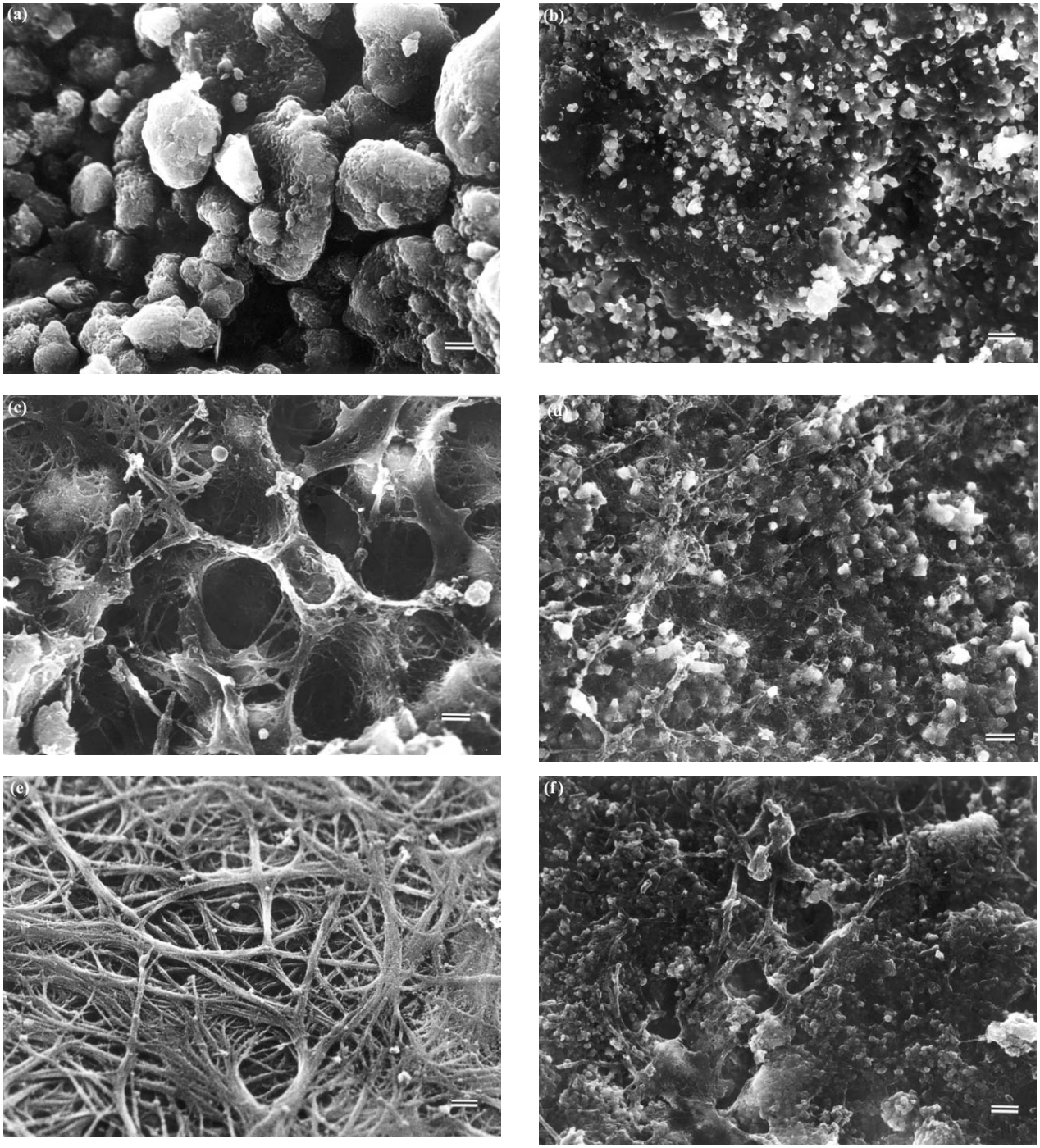

Figure 4 Scanning electron microscopy of the surface of the specimens. (a) The surface of the TiO_2 nanotube inserts before implantation. (b) The surface of the HA inserts before implantation. (c) Fine, immature fibers were present on the surface of the TiO_2 nanotube inserts on day 3. (d) The surface of the HA inserts had few fibers on day 3. (e) On day 7, the surface of the TiO_2 nanotube inserts had networks of fine fibers while the surface of the HA inserts (f) had very few fibers. Osteocytes were not normally present on the surface of the nonporous nanotube preparations, presumably because they were lost during the preparation for microscopy. The differences between the TiO_2 nanotube inserts and the HA inserts are much clearer on day 7 than on day 3 (bar = 1 μm).

ethanol and frozen on an aluminum plate chilled with liquid nitrogen and then cracked into two pieces by a chilled razor blade. The cracked specimens were dried and coated for SEM as described above.

For transmission electron microscopy (TEM), specimens were decalcified in K-CX for few days and then cut into small pieces. After fixation in 1% O_sO_4 cacodylate buffer solution overnight, they were dehydrated in graded ethanol that was replaced with acetone, and finally embedded in Epok 812 (Oken, Tokyo, Japan). Ultrathin sections were stained with uranyl acetate and lead citrate and observed with a JEM-1200 (JOEL, Tokyo, Japan) electron microscope at an accelerating voltage of 80 kV.

3. Results

3.1. Light microscopy

On day 3 after the operation, abundant spindle-shaped fibroblast-like cells were present between the bone matrix and the TiO_2 nanotubes (Fig. 1(a)). In contrast, few cells were present between the bone matrix and the

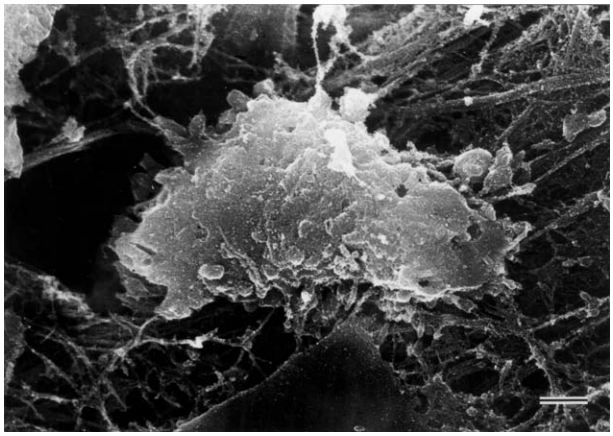

Figure 5 An osteoblast and fibers on the surface of a TiO_2 nanotube insert at day 7. The osteoblast was revealed by freeze cracking and is associated with fine fibers (diameter: 60–100 nm). This osteoblast had many processes and was a part of a monolayer located on the surface of the bone (bar = 1 μm).

HA insert (Fig. 1(b)) or β-TCP insert (Fig. 1(c)). On day 7, new bone formation in the porous TiO_2 nanotube inserts was apparent (Fig. 2). Cells that entered into the spaces of the nanotubes deposited new bone matrix that had the appearance of normal immature bone. Alkaline phosphatase positive cells were sandwiched between TiO_2 on one side and immature bone matrix on the other (Fig. 3).

3.2. Scanning electron microscopy

On day 3, fibers were present on TiO_2 nanotube inserts where none were present before implantation (Fig. 4(a) and (c)). In contrast, very new few fibers were observed on the surface of the HA inserts (Fig. 4(b) and (d)). This difference between TiO_2 nanotubes and HA became clearer on the day 7 (Fig. 4(e) and (f)) where 200 nm fibers were developed on the surface of the TiO_2 nanotube inserts but not on the HA inserts.

Freeze cracking on day 7 revealed osteoblasts and fibers on the surface of the TiO_2 nanotube inserts (Fig. 5). Backscattered electron imaging (BSE) showed bright areas that were much darker in the secondary electron imaging, indicating a thin layer of cells over the TiO_2 surfaces (Fig. 6).

3.3. Transmission electron microscopy

Transmission electron microscopy showed TiO_2 nanotubes near osteoblasts (Fig. 7). The nanotubes adhered to the extracellular matrix and not directly to the cells itself. Collagenous fibers were present beside the osteoblasts. Although a few histiocytes had apparently phagocytized some nanotubes, there were no inflammatory changes or inflammatory cells near the nanotubes and the osteoblasts.

4. Discussion

TiO_2 nanotubes have about three times the surface area of titanium oxide [5]. The increased surface area enhances the opportunities for interactions between the nanotubes and tissues around them. TiO_2 has numerous

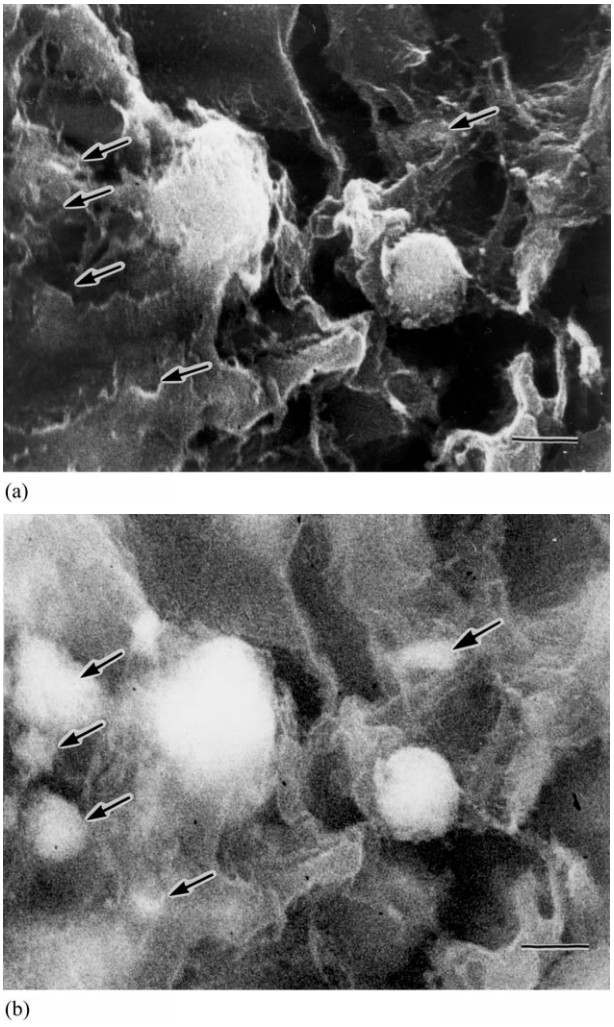

Figure 6 Scanning electron microscopy of the surface of the TiO_2 nanotubes on the day 7 by the method of freeze cracking. (a) Secondary electron imaging. (b) Backscatter electron imaging. TiO_2 nanotubes appear bright in the SEM image. The arrows in (a) and (b) indicate the same areas. The arrows of (a) indicate dark areas where organic material is on the surface. The arrows of (b) indicate bright areas showing the TiO_2 nanotubes underneath. Thus, there is thin layer of cells on the surface of the nanotubes (bar = 1 μm).

Ti–OH groups on its surface [3]. The basic Ti–OH groups induce apatite nucleation and crystallization in plasma-like fluids [7, 8]. In addition to Ti–OH [5, 6], the TiO_2 nanotubes in this study had Ca ions on their surfaces because $Ca(COO)_2$ was used for neutralization instead of HCl. Thus, the increased surface area with both Ti–OH and Ca-nucleation sites are likely to be the main reasons for the very rapid formation of bone-like apatite crystals.

On three days, TiO_2 nanotubes had fibroblast-like cells on their surfaces, while almost none were present on the surface of HA or β-TCP under the same conditions. The surfaces of TiO_2 nanotubes on days 3 and 7 also had more fibers compared to the other two inserts. These fibers are probably type I collagen produced by the osteoblasts [9–11].

Osteoblasts are the osteogenic cells that change into osteocytes, cells surrounded by the bone matrices [12, 13]. Preosteoblasts and osteoblasts are positive for alkaline phosphatase enzyme activity, while periosteal fibroblasts are negative [14]. On day 7, the cells associated with the TiO_2 inserts had the cytological

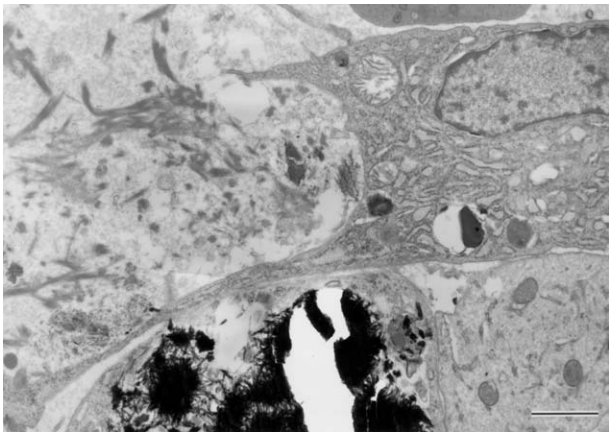

Figure 7 Transmission electron microscopy of an osteoblast associated with a TiO_2 nanotube insert. The osteoblast has typical well-developed rough endoplasmic reticulum and many processes extending from the surface. Collagenous fibers surround the cell. The TiO_2 nanotubes adhere to the extracellular matrix. There is no inflammatory reaction (bar = 1 μm).

characteristics of osteoblasts, including abundant rough endoplasmic reticulum, indented nucleus and scarce lysosomes [15, 16]. Thus, the collective observations by ALP stain, SEM and TEM are all consistent with the presence of osteoblasts near the TiO_2 nanotubes.

Freeze cracking, showed osteoblasts on fibers over the TiO_2 nanotubes. The difference between the backscatter electron images and the secondary electron images [17] clearly showed the existence of organic matter over the nanotubes. SEM showed that the surface of HA had small amounts of fibers and cells attached to it. These results are consistent with those of light microscopy.

Within seven days, TiO_2 nanotubes rapidly become coated with osteoblasts and regenerating new bone matrices. These developments occurred more rapidly than with HA [18] and β-TCP [19] that are currently used clinically in bone replacement procedures. TiO_2 nanotubes could be an efficient material for bone repair. Further study is needed to investigate the properties of TiO_2 nanotubes in bone regeneration over a longer period, such as several months.

5. Conclusions

New bone formation was observed in and around porous TiO_2 nanotube inserts in the femurs of Wistar rats after one week. TiO_2 nanotubes promote faster acquisition and development of osteoblasts and bone tissues and have better bone regenerating ability compared with clinically used HA and β-TCP.

References

1. B. KASEMO, *J. Prosthet. Dent.* **49** (1983) 832.
2. *IARC Monogr. Eval. Carcinog. Risks Hum.* **47** (1989) 307.
3. T. KASUGA, H. KONDO and M. NOGAMI, *J. Cryst. Growth* **235** (2002) 235.
4. T. KOKUBO, H. KUSHITANI and S. SAKKA, *J. Biomed. Mater. Res.* **24** (1990) 721.
5. T. KASUGA, M. HIRAMATSU, A. HOSON, T. SEKINO and K. NIIHARA, *Langmuir* **14** (1998) 3160.
6. T. KASUGA, M. HIRAMATSU, A. HOSON, T. SEKINO and K. NIIHARA, *Adv. Mater.* **11** (1999) 1307.
7. C. OHTSUKI, H. IIDA, S. HAYAKAWA and A. OSAKA, *J. Biomed. Mater. Res.* **35** (1997) 39.
8. P. LI, C. OHTSUKI, T. KOKUBO, K. NAKANISHI, N. SOGA and K. DE GROOT, *ibid.* **28** (1994) 7.
9. S. F. JACKSON, *Proc. R. Soc. B* **146** (1956) 270.
10. R. A. ROBINSON and M. L. WATSON, *Anat. Rec.* **114** (1952) 383.
11. R. A. ROBINSON and D. A. CAMERON, *J. Biophys. Biochem. Cytol.* **2** (1956) 253.
12. R. R. COOPER, J. W. MILGRAM and R. A. ROBINSON, *J. Bone Joint Surg. Amer.* **48-A** (1966) 1239.
13. B. L. SCOTT and M. D. GLIMCHER, *J. Ultrastruct. Res.* **36** (1971) 565.
14. J. J. PRITCHARD, *J. Anat.* **86** (1952) 259.
15. S. C. LUK, C. NOPAJAROONSRI and G. T. SIMON, *J. Ultrastruct. Res.* **46** (1974) 184.
16. E. A. TONNA, *Lab. Invest.* **31** (1974) 609.
17. M. SAITO, A. MARUOKA and T. MORI, *Biomaterials* **15** (1994) 156.
18. L. CERRONI, R. FILOCAMO, M. FABBRI, C. PICONI, S. CAROPRESO and S. G. CONDO, *Biomol. Eng.* **19** (2002) 119.
19. J. WILTFANG, H. A. MERTEN, K. A. SCHLEGEL, S. SCHULTZE-MOSGAU, F. R. KLOSS, S. RUPPRECHT and P. KESSLER, *J. Biomed. Mater. Res. (Appl. Biomater.)* **63** (2002) 115.

Received 20 August 2003
and accepted 8 January 2004